A Method for the Dynamic Analysis of the Heart Using a Lyapounov Based Denoising Algorithm

Jacinto C. Nascimento   João M. Sanches   Jorge S. Marques

Instituto de Sistemas e Robótica - Instituto Superior Técnico

Abstract— Heart tracking in ultrasound sequences is a difficult task due to speckle noise, low SNR and lack of contrast. Therefore it is usually difficult to obtain robust estimates of the heart cavities since feature detectors produce a large number of outliers. This paper presents an algorithm which combines two main operations: i) a novel denoising algorithm based on the Lyapounov equation and ii) a robust tracker, recently proposed by the authors, based on a model of the outlier features. Experimental results are provided, showing that the proposed algorithm is computationally efficient and leads to accurate estimates of the left ventricle during the cardiac cycle.

I. INTRODUCTION

The estimation of the left ventricle (LV) boundary is useful from a clinical point of view because it allows to extract relevant measures of the heart dynamic behavior, among which we stress the ejection fraction or local wall motion.

Ultrasound imaging, is one of the most used techniques to observe the dynamics of the heart. However, the low signal-to-noise ratio (SNR) and the multiplicative nature of the noise (speckle) corrupting the ultrasound images, make the LV segmentation a difficult task.

Edge detection algorithms fail due to the presence of multiplicative noise in heart ultrasound images. The strongest edges are often not located on the endocardium (in some cases, there are no visual cue for the presence of the myocardium border). In [1] it is proposed the instantaneous coefficient of variation (ICOV) providing good segmentation results, but the so called problem of "edge dropout" still remain (particularly in the diastole phase).

Therefore, noise reduction must be applied before edge detection. Several techniques have been proposed to reduce the speckle noise without distorting the relevant clinical details, e.g., Bayesian methods [2,3], mixture distribution of the Rician pdf with the inverse Gaussian as a mixture distribution (RiIG) [4], soft thresholding [5], wavelet based methods [6], wavelet soft-shrinking [7], or multiresolution based techniques [8], median filtering [9], and anisotropic diffusion [10].

Even though the denoising algorithms significantly reduce the speckle noise, advanced tracking techniques are needed to segment the LV boundaries. Prior art in segmentation of echocardiographic sequences of the heart includes active shape models [11,12], active contours [13] and level set techniques [14]. Pairs of coupled contours have also been used. The update methods use geometric restrictions (e.g., subspace shape model), dynamic models and the measurements models e.g., using heteroscedastic noise [15].

In this paper we join a novel denoising algorithm based on the Lyapounov equation and a recent robust tracker [16]. The denoising algorithm must to process a large number of ultrasound images in an efficient way [17]. This is obtained showing that the solution of the filtering process verifies a Lyapunov equation, which can be efficiently by known algorithms.

The robustness of the tracker is obtained by using middle level features (strokes), which are labelled as valid or invalid. Since the labels are unknown they are replaced by their probabilities computed using a probabilistic model of the observations. A data association filter is then used to update the contour parameters under the presence of outliers.

The tracking algorithm proposed in the paper was assessed using a set of image sequences, segmented by medical doctors. These images, are used as a ground truth to compute FOM (figures of merit). The performance of the tracker computed in this way is compared with other tracking algorithms.

The paper is organized as follows: Section II describes the overall system. Sections III, IV and V describe the pre-processing, feature detection and tracking steps respectively. Section VI describes experimental and section VII concludes the paper.

II. SYSTEM OVERVIEW

The proposed system aims is to track the boundary of the left ventricle during the cardiac cycle. The system input is a sequences of ultrasound images sampled at 25Hz.

The system performs three main operations (see Fig. 1); i) *denoising:* to reduce the speckle noise and enhance the contrast; due to the large amount of data to be processed a novel algorithm was developed to perform this task, ii) *feature detection:* detects intensity transitions along orthogonal lines to the contour (see Fig. 2). Transitions are obtained by applying a matched filter to the intensity profiles and computing the local maxima [18], and iii)*tracking* based on a robust tracking algorithm which fits a deformable curve to the points detected in the image. This algorithm must be able to deal with a large number of outliers and to interpolate the boundary when no features are detected due to low contrast of the heart boundary. This is specially important close to the apex and in the presence of sudden motion changes (e.g., in the mitral valve). A recent tracking algorithm is used in this step.

Fig. 1.   System overview.

III. PRE-PROCESSING

The performance of the tracker depends on the signal to noise ratio, SNR, of the input images. The images have a low SNR due to the presence of multiplicative noise (speckle). The speckle noise is modeled with a Rayleigh distribution with space varying parameter [19].

The goal of the pre-processing step is to reduce the noise without losing relevant information. In this paper a MAP criterion is used to estimate the original images from the noisy observations. This approach, however, is slow and computationally demanding. This difficulty is particulary severe in the present problem because we are dealing with a large number of ultrasound images.

In this paper we use a fast MAP denoising algorithm. The denoising algorithm estimates the original image, F, by minimizing the following energy function

$$E(Y, F) = -\log(p(Y|F)p(F)) \tag{1}$$

where Y is the noisy image, $p(Y|F)$ is the observation model and $p(F)$ is the prior distribution of the unknown image.

Assuming conditional independence of the observations, at different sites, we have $p(Y|F) = \prod_{ij}^{N,M} p(y_{ij}|f_{ij})$ where $p(y|f) = \frac{y}{f}e^{-y^2/2f}$ is the Rayleigh distribution.

Concerning the prior, a Gibbs density function with quadratic potential functions is used, i.e.,

$$p(F) = \frac{1}{Z}e^{-\alpha \sum_{p,q \in S}(f_p - f_q)^2} \tag{2}$$

where (p,q) are neighboring nodes, defined in the neighboring system S. α is a parameter and Z is a partition function.

The most probable solution is obtained by finding the global minimum of $E(Y,F)$. This task is usually difficult and time consuming. Therefore, here, we will find a sub-optimal solution which assumes that the MAP solution is a filtered version of the maximum likelihood solution.

The maximum likelihood estimates is obtained by solving

$$F^{ML} = \arg \min_X p(Y|F) \qquad (3)$$

which leads to

$$f_k^{ML} = \frac{y_k^2}{2} \qquad (4)$$

where f_k^{ML} is the kth pixel of image F^{ML}.

The smooth version of the ML estimates, is obtained by solving the following quadratic problem

$$\hat{F}_k = \arg \min_F \left[\|F - F^{ML}\|^2 + \alpha \|\Delta F\|^2 \right] \qquad (5)$$

where $\|\Delta F\|^2$ is the sum of all square diferences between neighboring nodes. $\|\Delta F\|^2$ is an approximation of the energy of the gradient and therefore the minimizer of (5) is a smooth version of F^{ML}, where the degree of smoothing is controlled by the parameter α.

The energy function to be minimized can be written as follows

$$
\begin{aligned}
E(F) &= trace \left[(F - F^{ML})^T (F - F^{ML}) \right] + \\
&\quad \alpha \quad trace \left[(\theta_v F)^T (\theta_v F) + (F\theta_h)^T (F\theta_h) \right]
\end{aligned} \qquad (6)
$$

where θ_v and θ_h are $n \times n$ vertical and $m \times m$ horizontal difference operators respectively. The stationary point of $E(F)$ can be found by solving

$$\nabla_F E(F) = F - F^{ML} + \alpha(\phi_v F + F\phi_h) = 0 \qquad (7)$$

where $\phi_v = \theta_v^T \theta_v$ and $\phi_h = \theta_h^T \theta_h$. After straightforward manipulations we obtain

$$\mathcal{A}F + F\mathcal{B} + Q = 0 \qquad (8)$$

where $\mathcal{A} = 0.5I_n + \alpha\phi_v$, $\mathcal{B} = 0.5I_m + \alpha\phi_h$ and $Q = -F^{ML}$. I_n and I_m are n and m dimensional identity matrices respectively.

The equation (8) is the so called Sylvester equation for which there are efficient algorithms available in several scientific packages, e.g., MatLab [20,21]. Fig.2 shows an example of de-noised ultrasound image using the
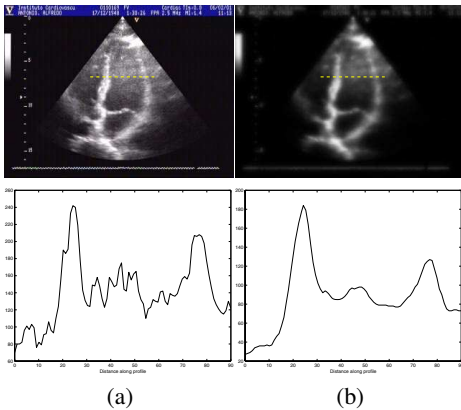

Fig. 2. Image profile taken at the dashed line: (a) without (b) with denoising.

pre-processing described above. This 320×240 dimensional image was obtained in about 5 seconds using the function $lyap(\mathcal{A}, \mathcal{B}, Q)$ from the MatLab package in a 2.8GHz Pentium 4 processor.

IV. FEATURE DETECTION

Feature detection aims to detect line segments belonging to the boundary of the LV. This is done in two steps. First we detect intensity transitions along lines orthogonal to the predicted contour (see Fig. 3). This is done by template matching. Feature detection along the ith direction is performed by computing the local minima of the function

$$\mathcal{J}(t_0) = \int_t |p_i(t) - T(t,t_0)|^2 dt \qquad (9)$$

where $p_i(t)$ is the image profile taken at the ith direction, t denotes the distance to the object boundary and $T(t,t_0)$ is a template which is obtained previously. The template T is obtained as follows: $T(t)$ is equal to the typical intensity of the object for $t \leq t_0$ and $T(t)$ is equal to the background intensity for $t > t_0$. Afterwords, feature points detected at consecutive lines are linked, forming image strokes.
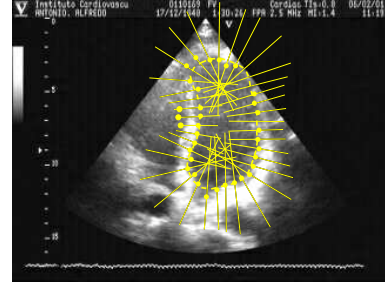

Fig. 3. Feature detection along orthogonal lines.

V. TRACKING

A deformable curve (B-spline) is used to approximate the LV contour. The parameters of the B-spline are estimated from the image features obtained in the previous step using a tracking algorithm.

This is not an easy task since the tracker should be able to classify the features as valid and invalid and track the contour using the invalid features only. The Kalman filter fails in this problem since it is not able to separate valid features from invalid ones.

In this paper we have used a data association filter called S-PDAF which was recently proposed in [16]. This computes the probabilities of each observation being valid using probabilistic models for the valid data and outliers.

To avoid an exponential growth of hypothesis a simplifying assumption is adopted: it is assumed that the state distribution given past observations is Gaussian i.e.,

$$p[x_k \mid Y^{k-1}] = \mathcal{N}[x_k; \hat{x}_{k|k-1}, P_{k|k-1}] \qquad (10)$$

where $\hat{x}_{k|k-1}$, $P_{k|k-1}$ are the mean and covariance of x_k given past observations Y^{k-1}.

The computation of the state estimate and uncertainty (state mean and covariance matrix) given current and past observations, are given as follows

$$\hat{x}_{k|k} = \hat{x}_{k|k-1} + \sum_{i=1}^{m_k} \alpha_{i\,k} K_{i\,k} \nu_{i\,k} \qquad (11)$$

which is in fact similar to the Kalman filter. The only difference is that we shall consider multiple data hypothesis (in (11) we have m_k data hypothesis). This is because we do not know which features belong to the object contour or not. Fig. 3 display an example where we already seen that some features belong or not to the left ventricle boundary. Thus, for each stroke two labels are assigned: "1" which accounts for valid segment; "0" which accounts for invalid one. Since the number of label can be high, the features are grouped in segments (strokes) reducing the labeling procedure.

In (11) $\hat{x}_{k|k}$ is the state vector $K_{i\,k}$, $\nu_{i\,k}$ are the Kalman gain and the innovation respectively as in Kalman filter, and $\alpha_{i\,k}$

$$\alpha_{i\,k} \triangleq p(H_{i\,k} \mid Y^k) \qquad (12)$$

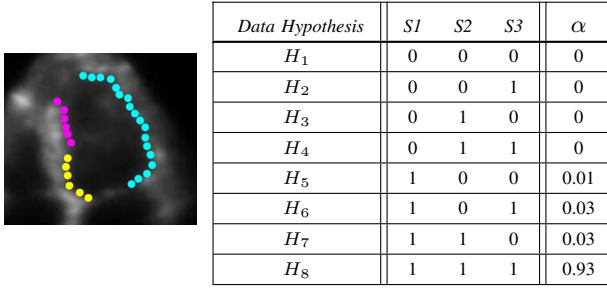| Data Hypothesis	S1	S2	S3	α
H_1	0	0	0	0
H_2	0	0	1	0
H_3	0	1	0	0
H_4	0	1	1	0
H_5	1	0	0	0.01
H_6	1	0	1	0.03
H_7	1	1	0	0.03
H_8	1	1	1	0.93

Fig. 4. Data Hypothesis and association probabilities.

is the *a posteriori* probability of the i-th hypothesis $H_{i\,k}$. The interpretation of equation (11) suggests that we have a bank of Kalman filters each one specialized to each ith data hypothesis. Fig. 4 illustrates, in a simple way, the idea of multiple data hypothesis. In this figure we can see three grouping features (each color refers to a different grouping feature), all belonging to the boundary of the left ventricle. In this case we have eight data hypothesis ($m_k = 8$). From this figure we concluded that all the grouping features contribute in a significant way to represent the outer boundary, having a weight $\alpha_{8\,k} = 0.93$.

A recursive equation can also be derived for the covariance matrix (see details in [16]).

$$P_{k|k} = \left[I - \sum_{i=1}^{m_k} \alpha_{i\,k} K_{i\,k} C_i\right] P_{k|k-1} + \sum_{i=0}^{m_k} \alpha_{i\,k} \hat{x}_{i\,k|k} \hat{x}_{i\,k|k}^T - \hat{x}_{k|k} \hat{x}_{k|k}^T$$

(13)

VI. Experimental Results

This section shows experimental results obtained with the proposed tracker Three echocardiographic sequences of the left ventricle were used in this study. Each sequence was obtained from a different patient. The sequences lengths are: 450 images (25 cardiac cycles), 490 images (26 cardiac cycles), 470 images (19 cardiac cycles) and each image has 320×240 pixels.

The experiments involve three steps: i) the LV boundary was manually defined by an expert in several images; ii) all sequences were automatically processed by the tracking algorithm proposed in the paper; iii) metrics between automatic and manual boundaries are computed for all the sequences. The tests were performed under three options: no preprocessing, median filtering preprocessing and Lyapounov pre-processing.

A. Ground Truth

We now describe the procedure to obtain the ground truth. An observer provides a hand-labelled contours for the sequences. Four images in each cardiac cycle are selected for hand labelling: two images in the systole phase and other two images in the diastole phase. A total number of 312 contours were manually generated (156 in each phase) for the three sequences. The computer-generated boundaries (provided by the S-PDAF tracker), are compared to the ground truth resulting in an error measurement in each image.

B. Error Metrics

Shape metrics to compare computer-generated boundaries against the boundaries outlined by the observer are now described.

The two curves are represented as sets of points $\mathcal{X} = \{\mathbf{x}_1, \mathbf{x}_2, \ldots, \mathbf{x}_{N_x}\}$, and $\mathcal{Y} = \{\mathbf{y}_1, \mathbf{y}_2, \ldots, \mathbf{y}_{N_y}\}$, where $N_y > N_x$. Each $\mathbf{x}_i$ and $\mathbf{y}_i$ is a pair of coordinates of the point in the image plane.

The distance from a point $\mathbf{x}_i$ to the curve $\mathcal{Y}$ is

$$d(\mathbf{x}_i, \mathcal{Y}) = \min_j ||\mathbf{y}_j - \mathbf{x}_i||$$

(14)

The average distance from the contour model $\mathcal{X}$ to the ground truth boundary $\mathcal{Y}$ (ideal contour) is

$$d_{av} = \frac{1}{N_x} \sum_{i=1}^{N_x} d(\mathbf{x}_i, \mathcal{Y})$$

(15)

The Hausdorff distance between the two curves is defined as the maximum distance from a point to the other curve [22]

$$d_{max}(\mathcal{X}, \mathcal{Y}) = \max\left(\max_i\{d(\mathbf{x}_i, \mathcal{Y})\}, \max_j\{d(\mathbf{y}_j, \mathcal{X})\}\right)$$

(16)

Another metric which we use to measure the distortion between two curves is based on the regions inside the two curves as proposed in [23] in the context of ultrasound image segmentation. This metric is defined by

$$d_H = \frac{\sharp\big((X \cup Y) - (X \cap Y)\big)}{\sharp(X \cup Y)}$$

(17)

where X, Y are binary images such that all pixels inside the curves have label 1 and all the other pixels have label 0. This metric computed the number of pixels which receive different labels and normalize it.

Fig. 5 shows the evolution of the metrics sequence. The first measure (column (a) of the figure) belongs to the interval $[0, 1]$, the remaining ones are expressed in terms of pixels. The dashed line refers to the results obtained by using a median filter in the pre-processing step. The solid line represents the values obtained by the proposed method. We do not show the metric for the estimated obtained without pre-processing since the results are much worse. Fig. 5 shows the results at specific frames. These frames corresponds to the time instants when the cardiac phase switch from systole to the diastole and vice-versa. This figure also depicts the situation when the tracker has difficulties to represent the *apex* of the ventricle.

Fig. 5 shows that the denoising technique proposed herein has a better performance compared with the median filter (the solid line is under the dashed line) most of the time. The second order statistics of the contour metrics are shown in Tables I, II, III. Table IV shows the average computation time associated to the tracker in seconds. We conclude that the proposed pre-processing method has three advantages: i) the mean error of the shape estimates is smaller than in the other cases; ii) the variance of the error is (slightly) smaller and iii) allows a faster tracking since less outlier features are detected in the image.

Fig. 6 show the number of outliers in each frame (for the sake of clarity 10% of the outliers frames are shown) for the case of the first sequence shown in Fig. 5.
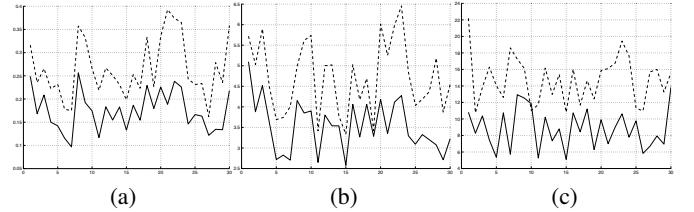

(a)   (b)   (c)

Fig. 5. Metrics statistics for the first sequence, (a) d_H, (b) d_{av}, (c) d_{max}.

	without	Median	Lyapounov
$\mathbf{E}[d_H]$	0.25	0.21	**0.16**
$\mathbf{var}[d_H]$	0.007	0.004	**0.002**
$\mathbf{E}[d_{av}]$	4.49	3.94	**3.42**
$\mathbf{var}[d_{av}]$	1.31	0.74	**0.47**
$\mathbf{E}[d_{max}]$	12.86	11.18	**8.80**
$\mathbf{var}[d_{max}]$	18.63	13.10	**9.64**

TABLE I

Mean and variance values for the metrics shown in the Fig. 5.

VII. Conclusions

This paper proposes a system for the tracking of the left ventricle using two key operations. The first is a novel denoising algorithm based on the

	without	Median	Lyapounov
$\mathbf{E}[d_H]$	0.20	0.17	**0.14**
$\mathbf{var}[d_H]$	0.004	**0.001**	**0.001**
$\mathbf{E}[d_{av}]$	3.88	3.86	**3.22**
$\mathbf{var}[d_{av}]$	1.21	0.76	**0.65**
$\mathbf{E}[d_{max}]$	10.32	11.36	**9.18**
$\mathbf{var}[d_{max}]$	17.51	17.53	**17.13**

TABLE II

MEAN AND VARIANCE VALUES FOR THE METRICS FOR THE SECOND SEQUENCE.

	without	Median	Lyapounov
$\mathbf{E}[d_H]$	0.21	0.17	**0.14**
$\mathbf{var}[d_H]$	0.014	0.004	**0.002**
$\mathbf{E}[d_{av}]$	4.41	3.22	**2.86**
$\mathbf{var}[d_{av}]$	11.6	0.81	**0.52**
$\mathbf{E}[d_{max}]$	12.25	8.40	**7.39**
$\mathbf{var}[d_{max}]$	98.20	10.9	**7.41**

TABLE III

MEAN AND VARIANCE VALUES FOR THE METRICS FOR THE THIRD SEQUENCE.

	without	Median	Denoising
Time_{av}	1.11	0.94	**0.76**
Time_{av}	0.99	0.91	**0.83**
Time_{av}	0.87	0.86	**0.76**

TABLE IV

TIME AVERAGE PER FRAME (VALUES IN SECONDS) FOR ALL THE SEQUENCES.

Lyapounov equation. The second is a robust tracker used to estimate the evolution of the LV contour during in cardiac sequences. It is assumed that some of the observations are outliers. Since we do not know which ones are valid a probabilistic labeling is performed, based on a model of the outlier features, and a data association filter is then used to update the LV contour.

It is concluded from the experimental results that the proposed algorithm manages to accurately track the heart motion in many ultrasound images with a low contrast between the heart cavity and the miocardium. It is also concluded that the denoising algorithm plays an important role and significantly reduces the number of outliers.
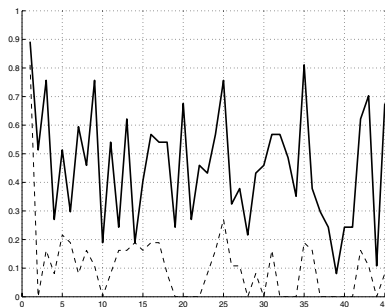

Fig. 6. Number of outliers of the sequence shown in Fig. 5. Without pre-processing (bold line) and with the proposed technique (dashed line).

REFERENCES

[1] Y. Yu and S. T. Acton, "Edge detection in ultrasound imagery using the instantaneous coefficient of variation," *IEEE Trans. Med. Imag.*, vol. 13, no. 12, pp. 1640–1655, December 2004.
[2] Z. Zeng and I. Cumming, "Bayesian speckle noise reduction using the discrete wavelet transform," in *Int. geoscience and remote sensing symposium*, july 1998, pp. 6–10.
[3] J. M. Dias, T. M. Silva, and J. Leitão, "Adaptive restoration of speckled SAR images using a compound random markov field," in *IEEE Int. Conf. on Image Processing*, vol. 2, 1998, pp. 79–83.
[4] T. Eltoft, "Modeling the amplitude statistics of ultrasonic images," *IEEE Trans. Med. Imag.*, vol. 25, no. 2, pp. 229–240, February 2006.
[5] S. Gupta, L. Kaur, R. C. Chauhan, and S. C. Saxena, "A wavelet based statistical approach for speckle reduction in medical ultrasound images," in *Medical and Biological Engineering and computing*, vol. 42, 2004, pp. 189–192.
[6] I. Duskunovic, A. Pizurica, G. Stippel, W. Philips, and I. Lemahieu, "Wavelet based denoising techniques for ultrasound images," in *Proc. of the IEEE Engineering in Medicine and Biology Society Conference*, vol. 4, 2000, pp. 2662–2665.
[7] Y. Yue, M. M. Croitoru, A. Bidani, J. B. Zwischenberger, and J. W. Clark, "Ultrasonic speckle suppression using robust nonlinear wavelet diffusion for lv volume quantification," in *Proc. of the 26th Annual Int. Conf. of the IEEE EMBS*, September 2004, pp. 1609–1612.
[8] A. Achim, A. Bezerianos, and P. Tsakalides, "Novel bayesian multiscale method for speckle removal in medical ultrasound images," *IEEE Trans. Med. Imag.*, vol. 20, no. 8, pp. 772–783, August 2001.
[9] T. Loupas, W. McDicken, and P. Allan, "An adaptive weighted median filter for speckle suppression in medical ultrasonic images," *IEEE Transactions on Circuits and Systems*, vol. 36, pp. 129–135, January 1989.
[10] J. Montagnat, M. Sermesant, H. Delingette, G. Malandain, and N. Ayache, "Anisotropic filtering for model-based segmentation of 4d cylindrical echocardiographic images," *Pattern Recognition Letters - Special Issue on Ultrasonic Image Processing and Analysis*, vol. 24, pp. 815–828, February 2003.
[11] J. G. Bosch, S. C. Mitchell, B. P. F. Lelieveldt, F. Nijland, O. Kamp, M. Sonka, and J. H. C. Reiber, "Automatic segmentation of echocardiographic sequences by active appearance motion models," *IEEE Trans. Med. Imag.*, vol. 21, no. 11, pp. 1374–1383, 2002.
[12] X. H. amd N. Paragios and D. Metaxas, "Establishing local correspondences towards compact representation of anatomical structures," *Medical Imaging Computing and Computer-Assisted Intervention*, 2003.
[13] D. Linker and V. Chalana, "A multiple active contour model for cardiac boundary detection on echocardiographic sequences," *IEEE Trans. Med. Imag.*, vol. 15, pp. 290–298, 1996.
[14] S. Osher and N. Paragios, *Geometric Level Set Methods in Inaging, Vision and Graphics*. Springer Verlag, 2003.
[15] X. S. Zhou, D. Comaniciu, and S. Krishnan, "An information fusion framework for robust shape tracking," in *Int'l Workshop on Statistical and Computational Theories of Vision*, Nice, France, October 2003.
[16] J. Nascimento and J. S. Marques, "Robust shape tracking in the presence of cluttered background," *IEEE Trans. Multimedia*, vol. 6, no. 6, pp. 852–861, December 2004.
[17] J. Sanches and J. S. Marques, "A rayleigh reconstruction/interpolation algorithm for 3d ultrasound," *Pattern Recognition Letters*, vol. 21, pp. 917–926, 2000.
[18] A. Blake and M. Isard, *Active Contours*. Springer, 1998.
[19] C. Burckhardt, "Speckle in ultrasound b-mode scans," *IEEE Trans. on Sonics and Ultrsonics*, vol. SU-25, no. 1, pp. 1–6, January 1978.
[20] R. Bartels and G. Stewart, "Solution of the matrix equation a x + xb = c," *Comm. A.C.M.*, vol. 15, pp. 820–826, 1972.
[21] A. Barraud, "A numerical algorithm to solve a xa - x = q." *IEEE Trans. Auto. Contr.*, vol. AC-22, pp. 883–885, 1977.
[22] D. P. Huttenlocher, G. A. Klanderman, and W. J. Rucklidge, "Comparing images using Hausdorff distance," *IEEE Trans. Pattern Anal. Machine Intell.*, vol. 15, pp. 850–863, 1993.
[23] A. Hammoude, "Computer-assited endocardial border identification from a sequence of two-dimensional echocardiographic images," Ph.D. dissertation, Univ. Washington, Seattle, WA, 1988.